Available online at www.worldscientificnews.com

World Scientific News

An International Scientific Journal

WSN 139(2) (2020) 135-154 EISSN 2392-2192

Thermal assessment of a convective porous moving fins of different material properties using Laplace-variational iterative method

M. G. Sobamowo[1,a], O. M. Kamiyo[1, b], M. O. Salami[1,2,c], A. A. Yinusa[1,d]

[1]Department of Mechanical Engineering, University of Lagos, Akoka, Lagos State, Nigeria

[2]Federal Institute of Industrial Research Oshodi, Lagos-State, Nigeria

[a-d]E-mail address: mikegbeminiyiprof@yahoo.com , omkamiyo@unilag.edu.ng , muhammedsalami22@gmail.com , aayinusa@unilag.edu.ng

ABSTRACT

Investigation on thermal responses of different materials subjected to variant environmental condition has been a subject of ever-increasing research interest for decades. As such, research studies have shown different materials exhibiting peculiar characteristics of commercially used heat enhancement devices. Therefore, this work presents an investigation on thermal behaviour of a convective porous moving fins with temperature dependent thermal conductivity for five different materials. These materials include copper, Aluminium, Silicon nitride, Silicon carbide and Stainless steel. A hybrid method, viz- Laplace-variational iterative method (LVIM) is used to solve the model equation developed. And a perfect agreement is achieved when the result obtained from LVIM is verified with the exact solution. The result obtained shows that silicon carbide compete favourably with copper as the most efficient material in heat enhancement, while stainless steel shows the least performance. It is hoped that this work will serve as a template and a helpful tool for both scientist and engineers' in future design of fins.

***Keywords*:** Thermal response, Variable thermal conductivity, Laplace-variational iterative method, variational iterative method, Exact Method

(Received 12 November 2019; Accepted 07 December 2019; Date of Publication 08 December 2019)

1. INTRODUCTION

The efficient dissipation of heat from devices in a thermal system is a critical factor determining the durability as well as the shelf-life of the components within the system and this is often achieved through the use of extended surfaces known as fin. As such, fins find application in many field of engineering practices, such as in Electronics, Power plant-, Thermal-, Aviation-, Chemical- , Nuclear Industries etc., to mention but few [1]

An overview of earlier work reveals an extensive studies carried out to investigate the thermal response of fins subjected to variant environmental conditions. Thus, Roy and Mallick, [2] carried out analysis of straight rectangular fins using Homotopy perturbation methods. The result obtained for optimum dimensionless parameter, efficiency and temperature distribution are suitable for practical fin. Hatami and Ganji [3], analytically determined the optimization of the longitudinal fins with different geometries, so as to determine the point at which the heat transfer rate reaches the optimum value in fins at constant volume.

The research findings shows that maximum heat transfer decreases with increase in fin thickness ratio, also that, an increase in the convection coefficient power index(m) increases the optimum points for profile power index(n) of fin geometry and fin thickness. In the work of Chen et al. [4], an assessment of heat sink performance with respect to material savings was conducted on trapezoidal and rectangular fin. The study shows that the performance drop depends on the different fin tip to base ratio and that the performance difference between the two selected profiles are quite insignificant at low velocity region but picks up as the velocity increases.

A transient condition of fin effectiveness and efficiency on the position function of rhombus sectional area was carried out by Nugroho and Purwadi [5], and their findings shows that the greater the value of convective heat transfer coefficient, the smaller the efficiency and the effectiveness of the fin becomes, in addition, under the transient condition, the effectiveness and the efficiency of the fin are significantly affected by the parameters such as density, thermal diffusity, specific heat and conductive heat transfer coefficient of the fin material. An exploration of thermal analysis of convective straight fin with temperature dependent thermal conductivity and internal heat generation was studied by Ghasemi, et al. [6], with constants chosen from industrial fins using the differential transform method (DTM), the result obtained matches with that of numerical results when verified.

In the work of Singh et al. [7], a comparison of heat transfer rate was carried out between fins with rectangular extensions and that of trapezoidal, triangular and circular extensions, the analysis reveals a greater heat transfer was achieved through the use of rectangular extension due to its wider surface area. Reddy et al. [8], numerically and experimentally determined the steady state temperature distribution in a pin fin using finite element method. The result obtained is in good agreement when validated with the experimental work. Joel et al. [9] , modelled the effect of fin geometry on the cooling process of computer microchips and discovered that higher heat enhancement per unit volume, higher efficiency in heat dissipation and greater heat loss per number of fin is exhibited by triangular spine fin geometry as compared with that of pin and rectangular spine geometry.

Wangikar et al. [10], analysed the effect of geometry on heat transfer coefficient of notched fins attached to vehicle engine and discovered that fins with triangular notches exhibit highest heat enhancement as compared to that of other geometries. Jain *et al.* [11], investigated the effect of variation of fin geometries on heat transfer of fin, the result obtained shows the

triangular fin exhibiting highest temperature drop and heat transfer rate. Thomas [12], worked on the effect of first order two dimensional formulation on heat transfer in fin assemblies and found out that effect is only significant in bimetal strip assemblies while it is less in arrays of fin made of material of the same compositions.

Past work have shown the significant effect of porosity on the heat distribution in fin using different model. Meanwhile, Kiwan *et al*. [13, 14] were the pioneer of the concept of using the Darcy model to analyse heat transfer in porous fin materials [15] and found it to be very effective. In the same vane, Patel et al. [16], analytically derived the temperature distribution efficiency and effectiveness of longitudinal porous fin, using Adomian decomposition sumudu transform method (ADSTM). It was observed from the obtained result, that the temperature distribution decreases with increase in porosity and convection parameter of the fin. Ma et al. [17], simulated a combined conductive, convective and radiative heat transfer in a moving irregular porous fin of different materials and geometries, using spectral element methods and concluded that volume adjusted efficiency is the best tool to use to compare the efficiency of fins with different configurations. In addition, their findings shows copper materials having the highest heat enhancement properties while the stainless steel shows the least. In a related work carried out by Hatami and Ganji [18], the thermal behaviour of longitudinal convective radiative porous moving fin with different section shapes and ceramic materials SiC and Si_3N_4 is analysed. The result obtained shows silicon carbide having the highest temperature distribution, while silicon nitride showing the least. However the trend reverses, when heat transfer properties of the materials is examined. Silicon nitride depicts the highest transfer, followed by Aluminum, while silicon carbide shows the least heat transfer rate.

Over the years, researchers have developed different methods of solution to predict the thermal behaviour of fins subjected to different environmental conditions. Thus, Vahabzadeh *et al*. [19] carried out analytical investigation of porous pin fin with variable section in fully wet conditions by using the Least square method (LSM) to solve a non-linear equation derived from the physical model and verified the result obtained with numerical method (fourth order Runge-kutta) with a very good agreement. Furthermore, an optimisation of longitudinal fins with different geometries for increasing the heat transfer was done by Hatami and Ganji [20], using the Least square methods (LSM). The work establishes a direct relationship between convective coefficient power index (m) and optimum point for profile power index (n) for the fin geometries. Sobamowo [21] made a significant correction to the work of Patra and Saha Ray [22], who employed Homotopy perturbation sumudu transform to solve convective radial fin with temperature-dependent thermal conductivity of fractional order energy equation.

Zaidi and shahzad [23], presented an analytical solution of temperature distribution in a rectangular fins with variable temperature surface heat flux using Optimal Homotopy Asymptotic Method (OHAM) and concluded that the results obtained are simple, effective and easy to apply for fin design. Ghoshdastidar and Mukhopadhyay [24], obtained a numerical solution for transient heat transfer in a straight composite fin using Alternating Direction implicit (ADI), the result obtained shows good agreement with known analytical solution except for a small time and large distance.

Bhowmik, *et al.* [25], predicted the geometry of rectangular and hyperbolic fin profile with temperature dependent thermal properties using Adomian decomposition and differential evolutionary methods and this serves as platform of selection of rectangular and annular fin that can satisfy a given temperature field. A generalized Hankel transform is used for the thermal conduction analysis of a hollow cylinder in [26], the result obtained is verified with finite

element method with good agreement. The effectiveness of a New iterative method (NIM) in solving non- linear partial differential equations is expressed in [27, 28], with the result showing good agreement with the existing methods such as VIM, ADM, and HPM. In addition, it was found out that the method provides a convergent series with easily computable components as compared to other existing methods. In the investigation carried out by Su and Xu [29], Green function was used to analyse steady state heat distribution of a plate fin heat sink, the outcome of simulation show good agreement when validated with experimental measurement. Khan et al, [30], applied Homotopy Analysis Method [HAM] to analyse the thermal radiation effect on squeezing flow casson fluid between parallel disks and verified the result with numerical solution, which proves HAM as an effective tool in solving the physical model.

The aforementioned analysis reveals the depth of work done in the past, on evolution of methods of solution and its application in expressing the heat distribution in fins. While Refs (16-23, 25-27), show the strength of approximate analytical method, Refs (24) depicts that of numerical methods and the strength of exact method is shown in Refs (26 and 29). However, this work presents a hybrid method of solution, viz Laplace Variational iterative method in analysing the thermal behaviour of convective porous moving fins, since it has the advantage of combining the strength of both analytical as well as that of approximate analytical methods.

2. PHYSICAL MODEL

The heat transfer equation for the model is subjected to the following assumptions:

1. Steady state situation is assumed
2. The porous medium is isotropic, homogeneous and saturated with single fluid
3. Darcy law governs the interaction between the fluid and porous medium
4. There is no thermal resistance between the fin base and the solid and the fin tip is convective
5. The solid and fluid are in local thermal equilibrium
6. The thermal conductivity of the material varies with temperature by the following equation:

$$k = k_a[1+\gamma(\mathrm{T}-\mathrm{T}_\infty)] \qquad (1)$$

Based on the aforementioned assumptions, the energy equation for the physical model depicted in Fig. 1, above is expressed as:

Energy in the left face = Energy out right face + Energy lost by convection + Energy lost by moving + Energy lost by immersed fluid. …….. (2)

or

$$q_x = q_{x+dx} + q_{convection} + q_{moving} + q_{porous}$$

$$-\mathrm{kA}_c\frac{dT}{dx}=-\mathrm{kA}_c\frac{dT}{dx}+\frac{d}{dx}\left(-kA_c\frac{dT}{dx}\right)dx+hP(\mathrm{T}-\mathrm{T}_\infty)dx+\rho c_p u\frac{dT}{dx}dx+\frac{\rho gk\beta c_p P(\mathrm{T}-\mathrm{T}_\infty)^2dx}{\nu}$$

$$\frac{d}{dx}\left(-kA_c\frac{dT}{dx}\right)dx+hP(\mathrm{T}-\mathrm{T}_\infty)dx+\rho c_p u\frac{dT}{dx}dx+\frac{\rho gk\beta c_p P(\mathrm{T}-\mathrm{T}_\infty)^2dx}{\nu}=0$$

$$-kA_c\frac{d^2T}{dx^2}-A_c\frac{dT}{dx}\frac{dk}{dx}+hP(\mathrm{T}-\mathrm{T}_\infty)+\rho c_p u\frac{dT}{dx}+\frac{\rho gK\beta c_p P(\mathrm{T}-\mathrm{T}_\infty)^2}{\nu}=0 \qquad (3)$$

Substituting $k=k_a[1+\gamma(\mathrm{T}-\mathrm{T}_\infty)]$ in Eq. (3), gives,

$$-k_a[1+\gamma(\mathrm{T}-\mathrm{T}_\infty)]A_c\frac{d^2T}{dx^2}-A_c\frac{dT}{dx}\frac{d\left(k_a[1+\gamma(\mathrm{T}-\mathrm{T}_\infty)]\right)}{dx}+hP(\mathrm{T}-\mathrm{T}_\infty)+\rho c_p u\frac{dT}{dx}+\frac{\rho gK\beta c_p P(\mathrm{T}-\mathrm{T}_\infty)^2}{\nu}=0 \qquad (4)$$

$$\begin{aligned}&-k_aA_c(\mathrm{T}_b-\mathrm{T}_\infty)\frac{d^2\theta}{dx^2}-A_ck_a\gamma\theta(\mathrm{T}_b-\mathrm{T}_\infty)^2\frac{d^2\theta}{dx^2}-k_a\gamma A_c(\mathrm{T}_b-\mathrm{T}_\infty)^2\frac{d\theta}{dx}\frac{d\theta}{dx}\\&+hP\theta(\mathrm{T}_b-\mathrm{T}_\infty)+\rho c_p u(\mathrm{T}_b-\mathrm{T}_\infty)\frac{d\theta}{dx}+\frac{\rho gK\beta c_p P\theta^2(\mathrm{T}_b-\mathrm{T}_\infty)^2}{\nu}=0\end{aligned} \qquad (5)$$

By applying the following on Eq. (5) and simplify, we have;

$$x=\xi L,\quad u=UU_{\max}$$

$$\begin{aligned}&-\frac{d^2\theta}{d\xi^2}-\gamma\theta(\mathrm{T}_b-\mathrm{T}_\infty)\frac{d^2\theta}{d\xi^2}-\gamma(\mathrm{T}_b-\mathrm{T}_\infty)\frac{d\theta}{d\xi}\frac{d\theta}{d\xi}+\frac{hPL^2}{k_aA_c}\theta+\\&\frac{\rho c_pUU_{\max}L}{k_aA_c}\frac{d\theta}{d\xi}+\frac{\rho gK\beta c_pL^2\theta^2(\mathrm{T}_b-\mathrm{T}_\infty)}{k_aA_c\nu}=0\end{aligned} \qquad (6)$$

Substitute $\beta=\gamma(\mathrm{T}_b-\mathrm{T}_\infty)$ in Eq. (6), gives;

$$\frac{d^2\theta}{d\xi^2}+\beta\theta\frac{d^2\theta}{d\xi^2}+\beta\left(\frac{d\theta}{d\xi}\right)^2-\frac{hPL^2}{k_aA_c}\theta-\frac{\rho c_pUU_{\max}L}{k_aA_c}\frac{d\theta}{d\xi}-\frac{\rho gK\beta c_pL^2\theta^2(\mathrm{T}_b-\mathrm{T}_\infty)}{k_aA_c\nu}=0 \qquad (7)$$

By using the following non dimensional parameters on Eq. (7):

$$\theta=\frac{(T-T_\infty)}{(\mathrm{T}_b-\mathrm{T}_\infty)},\ U=\frac{u}{U_{\max}},\quad \xi=\frac{x}{L},\ \beta=\gamma(\mathrm{T}_b-\mathrm{T}_\infty),\ N_{cc}^2=\frac{hPL^2}{k_aA_c},$$

$$Pe=\frac{\rho c_pUU_{\max}L}{k_aA_c}\quad and\quad S_h=\frac{\rho gc_pk\beta L^2(\mathrm{T}_b-\mathrm{T}_\infty)^2}{\nu A_ck_a}$$

The non-dimensional form of the equation can be expressed as:

$$\frac{d^2\theta}{d\xi^2}+\beta\theta\frac{d^2\theta}{d\xi^2}+\beta\left(\frac{d\theta}{d\xi}\right)^2-N_{cc}^2\theta-Pe\frac{d\theta}{d\xi}-S_h\theta^2=0 \tag{8}$$

As shown in Fig: 1. The Boundary condition can be written as:

$$\frac{d\theta}{d\xi}\Big|_{\xi=0}=0$$
$$\theta\Big|_{\xi=1}=1 \tag{9}$$

In order to demonstrate the effectiveness of the porous moving fin, the efficiency of the fin is expressed as the ratio of actual heat transfer to the ideal heat transfer. The porosity parameter (S_h) is as it obtains in [17].

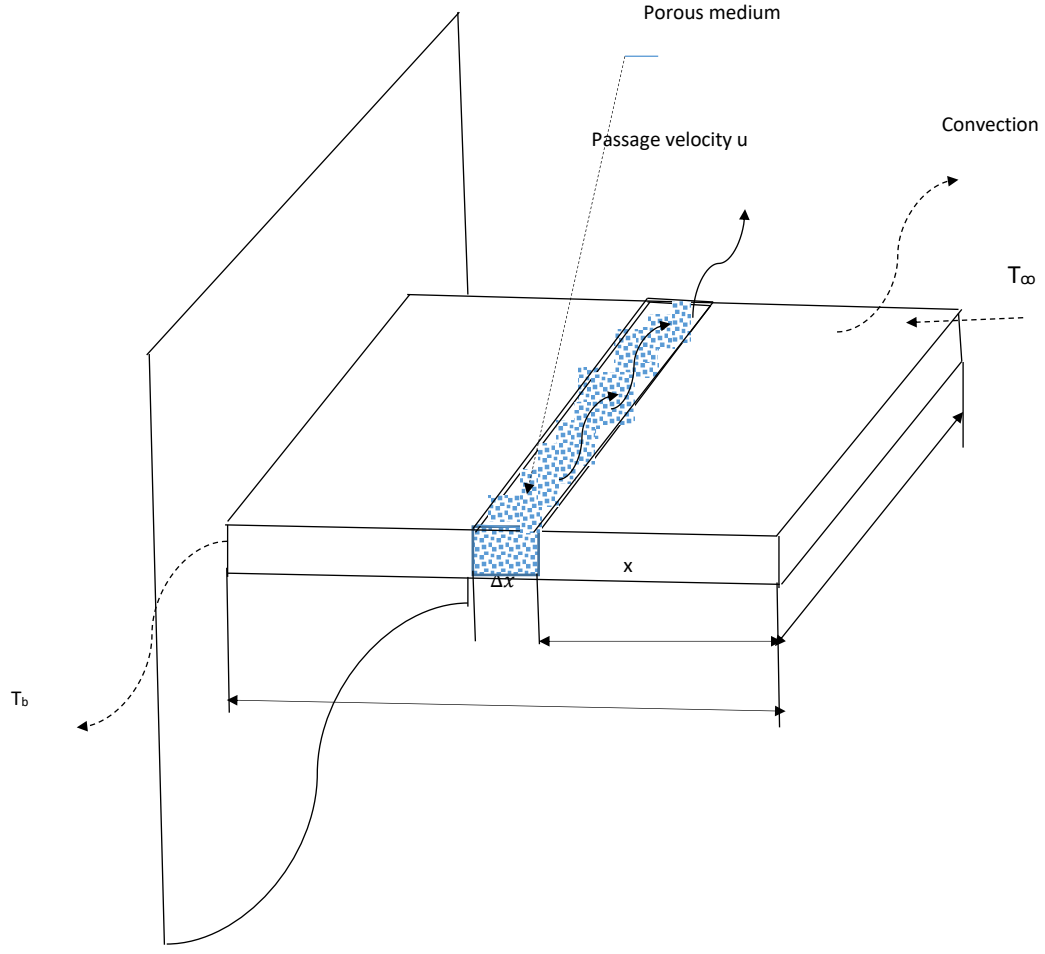

Fig. 1. showing the geometry of the moving porous fin

2. 1. Laplace variation iterative methods

This is a hybrid method of solution that combines the strength of exact method of solution, with that of an approximate analytical methods. This hybrid method is adopted in solving the governing equation expressed in Eq. (8), in order to have a closed form analytical expression.

The theory of Laplace variation iterative Method is expressed below:

Giving a typical Ordinary differential Equation shown in Eq. (8) below:

$$L\theta(\xi) + N\theta(\xi) = g(\xi) \tag{10}$$

where

L = linear operator, N = non-linear term and g(x) = source term.

The Lvim correction functional for Eq. (8) is expressed as:

$$\theta_{n+1}(\xi) = \theta_n(\xi) + \int_0^{\xi} \lambda(\xi)\left(L\theta_n(\varepsilon) + N\bar{\theta}_n(\varepsilon) - g(\varepsilon)\right)d\varepsilon \qquad n = 0,1,2..... \tag{11}$$

where $\lambda = lagrange\ multiplier,\ \bar{\theta}_n\ is\ the\ restricted\ \text{variation}\ of\ \delta\theta_n = 0$

The general form of Lagrange multiplier can be expressed as: $\lambda = \bar{\lambda}(\xi - \varepsilon)$

Applying Laplace properties on equation (8), we have:

$$\mathcal{L}[\theta_{n+1}(\xi)] = \mathcal{L}[\theta_n(\xi)] + \mathcal{L}\left[\int_0^{\xi} \lambda(\xi)\left(L\theta_n(\varepsilon) + N\bar{\theta}_n(\varepsilon) - g(\varepsilon)\right)d\varepsilon\right], \quad n = 0,1,2... \tag{12}$$

$$\mathcal{L}[\theta_{n+1}(\xi)] = \mathcal{L}[\theta_n(\xi)] + \mathcal{L}\left[\bar{\lambda}(\xi) * \left(L\theta_n(\varepsilon) + N\bar{\theta}_n(\varepsilon) - g(\varepsilon)\right)\right]$$

$$\mathcal{L}[\theta_{n+1}(\xi)] = \mathcal{L}[\theta_n(\xi)] + \mathcal{L}\left[\bar{\lambda}(\xi)\right]\mathcal{L}\left[\left(L\theta_n(\varepsilon) + N\bar{\theta}_n(\varepsilon) - g(\varepsilon)\right)\right] \tag{13}$$

Taking the variation of Eq. (13) with respect to $\theta_n(\xi)$, we obtain the optimal value of $\lambda = \bar{\lambda}(\xi - \zeta)$

$$\frac{\delta}{\delta\theta_n}\mathcal{L}[\theta_{n+1}(\xi)] = \frac{\delta}{\delta\theta_n}\mathcal{L}[\theta_n(\xi)] + \frac{\delta}{\delta\theta_n}\mathcal{L}\left[\bar{\lambda}(\xi)\right]\mathcal{L}\left[\left(L\theta_n(\varepsilon) + N\bar{\theta}_n(\varepsilon) - g(\varepsilon)\right)\right] \tag{14}$$

Applying variation on Eqn. (14), we have

$$\mathcal{L}[\delta\theta_{n+1}] = \mathcal{L}[\delta\theta_n] + \delta\mathcal{L}\left[\bar{\lambda}\right]\mathcal{L}[\theta_n] \tag{15}$$

The linear differential operator L has a constant coefficient given as:

$$\mathcal{L}\theta \text{ş } a_n\theta^{(n)} + a_{n-1}\theta^{(n-1)} + a_{n-2}\theta^{(n-2)} + ...a_2\theta'' + a_1\theta' + a_0\theta \tag{16}$$

Laplace transform of the first term of L operator

$$\mathcal{L}\left[a_n\theta^n\right] = a_n S^n \mathcal{L}[\theta] - a_n \sum_{k=1}^{n} S^{k-1}\,\theta^{(n-k)}(0) \tag{17}$$

so, the variation with respect to θ is given by:

$$\delta\mathcal{L}\left[a_n\theta^n\right] = a_n S^n \mathcal{L}[\delta\theta] \tag{18}$$

Also, terms $a_{n-1}\theta^{(n-1)} + a_{n-2}\theta^{(n-2)} + \ldots a_2\theta'' + a_1\theta' + a_0\theta$ yield similar results.
By using Eqn. (16), Eqn.(17) reduces to

$$\mathcal{L}[\delta\theta_{n+1}] = \mathcal{L}[\delta\theta_n] + \mathcal{L}[\bar{\lambda}]\left(\sum_{k=0}^{n} a_k S^k\right)\mathcal{L}[\delta\theta_n] = \left[1 + \mathcal{L}[\bar{\lambda}]\left(\sum_{k=0}^{n} a_k S^k\right)\right]\mathcal{L}[\delta\theta_n] \tag{19}$$

The extremum condition of θ_{n+1}, requires that $\delta\theta_{n+1}$ is set to zero. Therefore

$$\left[1 + \mathcal{L}[\bar{\lambda}]\left(\sum_{k=0}^{n} a_k S^k\right)\right]\mathcal{L}[\delta\theta_n] = 0$$

$$1 + \mathcal{L}[\bar{\lambda}]\left(\sum_{k=0}^{n} a_k S^k\right) = 0$$

$$\mathcal{L}[\bar{\lambda}] = -\frac{1}{\left(\sum_{k=0}^{n} a_k S^k\right)} \tag{20}$$

$$\bar{\lambda} = \mathcal{L}^{-1}\left(\frac{1}{\sum_{k=0}^{n} a_k S^k}\right)$$

By substituting the value of $\bar{\lambda}$ in Eq. (19), the following iterative expression is obtained:

$$\mathcal{L}[\theta_{n+1}(\xi)] = \mathcal{L}[\theta_n(\xi)] + \mathcal{L}\left[\int_0^{\xi} \bar{\lambda}(\xi)\left(L\theta_n(\varepsilon) + N\theta_n(\varepsilon) - g(\varepsilon)\right)d\varepsilon\right], \quad n \geq 0. \tag{21}$$

Application of Laplace-vim scheme on the governing Eq. (8) gives;

$$\mathcal{L}[\theta_{n+1}(\xi)] = \mathcal{L}[\theta_n(\xi)] + \mathcal{L}\left[\int_0^{\xi} \bar{\lambda}(\xi-\varepsilon)(\theta'' + \beta\bar{\theta}\bar{\theta}'' + \beta\bar{\theta}'^2 - N_{cc}^2\theta - Pe\theta' - S_h\bar{\theta}^2)d\varepsilon\right] \tag{22}$$

The iteration for n = 1 and n = 2, gives the temperature distribution solution below:

$$\theta_1(\xi) = \frac{A\left(-AS_h + Pe + \cosh\left(\sqrt{N_{cc}{}^2 + Pe}x\right)\left(AS_h + N_{cc}{}^2\right)\right)}{N_{cc}{}^2 + Pe} \tag{23}$$

$$\theta_2(\xi) = \left(\begin{array}{l} \dfrac{A^2 S_h}{6\left(N_{cc}{}^2 + Pe\right)^3}\left(\begin{array}{l} -9A^2S_h{}^2 + 3N_{cc}{}^4 + 6PeN_{cc}{}^2 - 6Pe^2 + 2\cosh\left(\sqrt{N_{cc}{}^2 + Pe}x\right)\left(\begin{array}{l} 4A^2S_h{}^2 + 2AN_{cc}{}^2S_h - 2N_{cc}{}^4 \\ -6APeS_h - 3PeN_{cc}{}^2 + 3Pe^2 \end{array}\right) \\ +\cosh\left(2\sqrt{N_{cc}{}^2 + Pex}\right)\left(AS_h + N_{cc}{}^2\right)^2 + 6AS_h\left(-N_{cc}{}^2 + 2Pe\right) \end{array}\right) \\ +\dfrac{A\left(AS_h + N_{cc}{}^2\right)}{2\left(N_{cc}{}^2 + Pe\right)^{5/2}}\left(A^2\beta xN_{cc}{}^2S_h + A^2Pe\beta xS_h - APe\beta xN_{cc}{}^2 - 2A^2xS_h{}^2 - APe^2\beta x \right.\\ \left. +2APexS_h - PexN_{cc}{}^2 - Pe^2x - PeN_{cc}{}^2 - Pe^2\right)\sinh\left(\sqrt{N_{cc}{}^2 + Pex}\right) \\ +\dfrac{A}{6\left(N_{cc}{}^2 + Pe\right)^2}\left(\begin{array}{l} 6Pe^2 + \cosh\left(\sqrt{N_{cc}{}^2 + Pex}\right)\left(\begin{array}{l} 2A^3\beta S_h{}^2 + 4A^2\beta N_{cc}{}^2S_h + 3APexN_{cc}{}^2S_h + 2A\beta N_{cc}{}^4 + 3PexN_{cc}{}^4 \\ +3APe^2xS_h + 3Pe^2xN_{cc}{}^2 + 6AN_{cc}{}^2S_h + 6N_{cc}{}^4 + 6APeS_h + 12PeN_{cc}{}^2 \end{array}\right) \\ -2A\left(\beta\left(AS_h + N_{cc}{}^2\right)^2\cosh\left(2\sqrt{N_{cc}{}^2 + Pex}\right) + 3S_h\left(N_{cc}{}^2 + Pe\right)\right) \end{array}\right) \end{array}\right) \tag{24}$$

2. 2. Fin Efficiency

This is defined as the ratio of actual heat transfer to the ideal heat transfer [17]. It is a measure of heat enhancement capacity of the fin.

$$\eta = \frac{Q_{actual}}{Q_{ideal}} \tag{25}$$

$$\eta = \frac{\int_0^1\left(hP(\mathrm{T}-\mathrm{T}_\infty) + \rho c_p UU_{\max}\dfrac{dT}{dx} + \dfrac{\rho gk\beta c_p\,\mathrm{P}(\mathrm{T}-\mathrm{T}_\infty)^2}{\nu}\right)dx}{hP(\mathrm{T}_b-\mathrm{T}_\infty) + \rho c_p UU_{\max}\dfrac{dT}{dx} + \dfrac{\rho gk\beta c_p A(\mathrm{T}_b-\mathrm{T}_\infty)^2}{\nu}}$$

$$\eta = \frac{\int_0^1\left(N_{cc}^2\theta + Pe\dfrac{d\theta}{d\xi} + S_h\theta^2\right)d\xi}{N_{cc}^2 + Pe\dfrac{d\theta}{d\xi} + S_h} \tag{26}$$

3. VERIFICATION OF LVIM

Table 1. Below, shows the verification of LVIM with exact solution of the physical model equation developed. It also reveal that LVIM predicts better than VIM.

Table 1. Non-dimensional temperature distribution in a longitudinal moving Porous fin for exact, VIM and LVIM. $\beta = 0,\ S_h = 0,\ Pe = 0.1$ *and* $N_{cc} = 0.1$

ξ	θ		
	Exact	VIM	LVIM
0.0	0.9948513885	0.9948513884	0.9948513885
0.1	0.9949012982	0.9949012976	0.9949012977
0.2	0.9950516980	0.9950516985	0.9950516987
0.3	0.9953036169	0.9953036161	0.9953036163
0.4	0.9956580964	0.9956580959	0.9956580961
0.5	0.9961162053	0.9961162048	0.9961162046
0.6	0.9966790300	0.9966790295	0.9966790297
0.7	0.9973476798	0.9973476797	0.9973476794
0.8	0.9981232856	0.9981232855	0.9981232860
0.9	0.9990070013	0.9990070001	0.9990070006
1.0	1.0000000000	0.9999999985	1.0000000000

Table 2. Thermo-physical properties of air the under ambient condition [17].

$\rho_f,\ kg.m^{-3}$	$k_f, Wm^{-1}k^{-1}$	$c_{pf,}\ Jkg^{-1}K^{-1}$	$v_{f,}\ m^2s^{-1}$	β, K
1.24	0.026	1005	1.568×10^{-5}	3.3×10^{-3}

Table 3. Thermo-physical properties of air the under ambient condition [17].

Materials	$\rho_s,\ kg.m^{-3}$	$k_s, Wm^{-1}k^{-1}$	$c_{ps,}\ Jkg^{-1}K^{-1}$
Aluminum	2700	235	897
Copper	8960	401	386
Silicon Nitride (Si_3N_4)	3200	25	500
Silicon Carbide (SiC)	3210	370	35
Stainless Steel	7930	16.3	491

3. 1. Exact Analytical Solution

The exact solution of any given equation is the actual solution of the linear part of the model equation and it stands as the benchmark by which the solution given by any other

methods, either approximate analytical methods or numerical methods are measured. In case of Eq. (8), the exact solution can be expressed as:

$$\theta(\xi) = A\mathrm{e}^{1/2xPe}\left(\cosh\left(1/2x\sqrt{Pe^2+4N_{cc}{}^2}\right) - \frac{Pe\sinh\left(1/2x\sqrt{Pe^2+4N_{cc}{}^2}\right)}{\sqrt{Pe^2+4N_{cc}{}^2}}\right) \tag{27}$$

3. 2. Variational iterative method (VIM) of solution

This is an approximate analytical method which are best used in solving non-linear equations in form of analytical expressions, it serves as an easy and helpful tools in designs for scientist and engineers.

$$\theta_2(\xi) = \begin{pmatrix} A - 1/2\left(-S_hA^2 - N_{cc}{}^2A\right)\xi^2 + 1/30S_h\left(1/2S_hA^2 + 1/2N_{cc}{}^2A\right)^2\xi^6 \\ +1/4\begin{pmatrix}\beta\left(1/2S_hA^2+1/2N_{cc}{}^2A\right)\left(S_hA^2+N_{cc}{}^2A\right)+\beta\left(-S_hA^2-N_{cc}{}^2A\right)^2 \\ -N_{cc}{}^2\left(1/2S_hA^2+1/2N_{cc}{}^2A\right)-2S_hA\left(1/2S_hA^2+1/2N_{cc}{}^2A\right)\end{pmatrix}\xi^4 \\ +1/3\left(-\xi\begin{pmatrix}\beta\left(1/2S_hA^2+1/2N_{cc}{}^2A\right)\left(S_hA^2+N_{cc}{}^2A\right)+\beta\left(-S_hA^2-N_{cc}{}^2A\right)^2 \\ -N_{cc}{}^2\left(1/2S_hA^2+1/2N_{cc}{}^2A\right)-2S_hA\left(1/2S_hA^2+1/2N_{cc}{}^2A\right)\end{pmatrix}+Pe\left(-S_hA^2-N_{cc}{}^2A\right)\right)\xi^3 \\ +1/2\left(-Pe\left(-S_hA^2-N_{cc}{}^2A\right)\xi+\beta A\left(S_hA^2+N_{cc}{}^2A\right)\right)\xi^2-\xi^2\beta A\left(S_hA^2+N_{cc}{}^2A\right) \end{pmatrix} \tag{28}$$

Other higher values of $\theta(\xi)$ are too big to be expressed here.

4. RESULT AND DISCUSSION

In this work, five different materials were selected in expressing the thermal analysis of the fin model equation developed. These materials are copper, Aluminum, silicon nitride, silicon carbide and stainless steel. A straight porous moving fin of regular rectangular geometry is used for the analysis and the dispersed medium is air governed by Darcy model [4, 5].

In Fig. 2, the temperature distribution against non-dimensional length is plotted for the solutions obtained from the exact-, variational iterative- and Laplace variational iterative methods and superimposed. The result shows that Laplace variational iterative method predicts more accurately and closer to the exact solution than the solution obtained from variational iterative method, as shown clearly in Table 1. Furthermore, Fig. 2b. Shows the expanded diagram of the graph.

The Effect of moving porous materials of copper, aluminum, silicon nitride, silicon-carbide and stainless steel on Non-dimensional Temperature distribution is shown in Fig.3, the curve displayed an increasing temperature distribution with increase in non-dimensional length, with copper material having the highest increase in non-dimensional temperature and the stainless steel having the least. The reason for this can be linked to the thermal conductivity properties of each of the materials, as depicted in Table. 1.

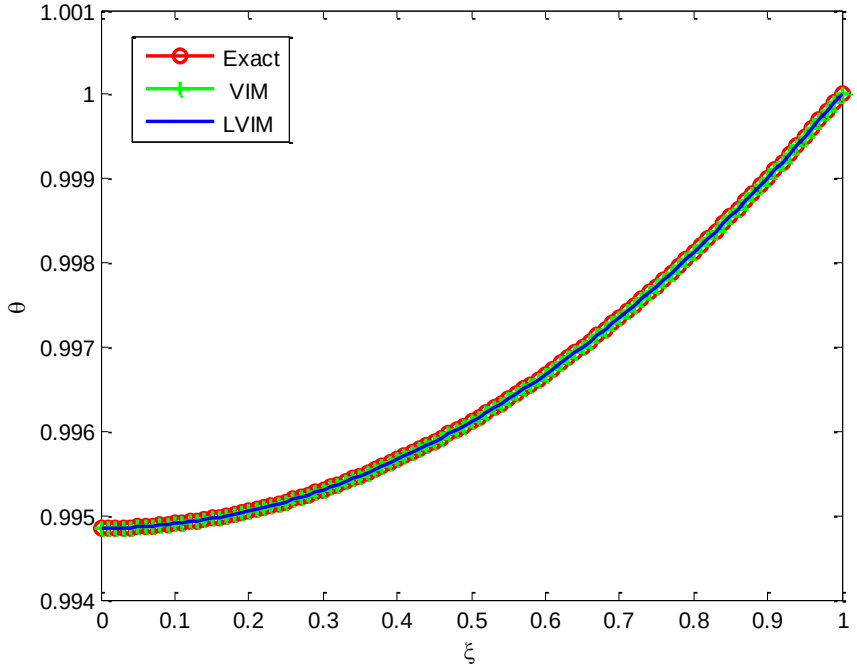

Fig. 2. Temperature distribution against Non-dimensional length for Exact-, Vim-, and Lvim methods

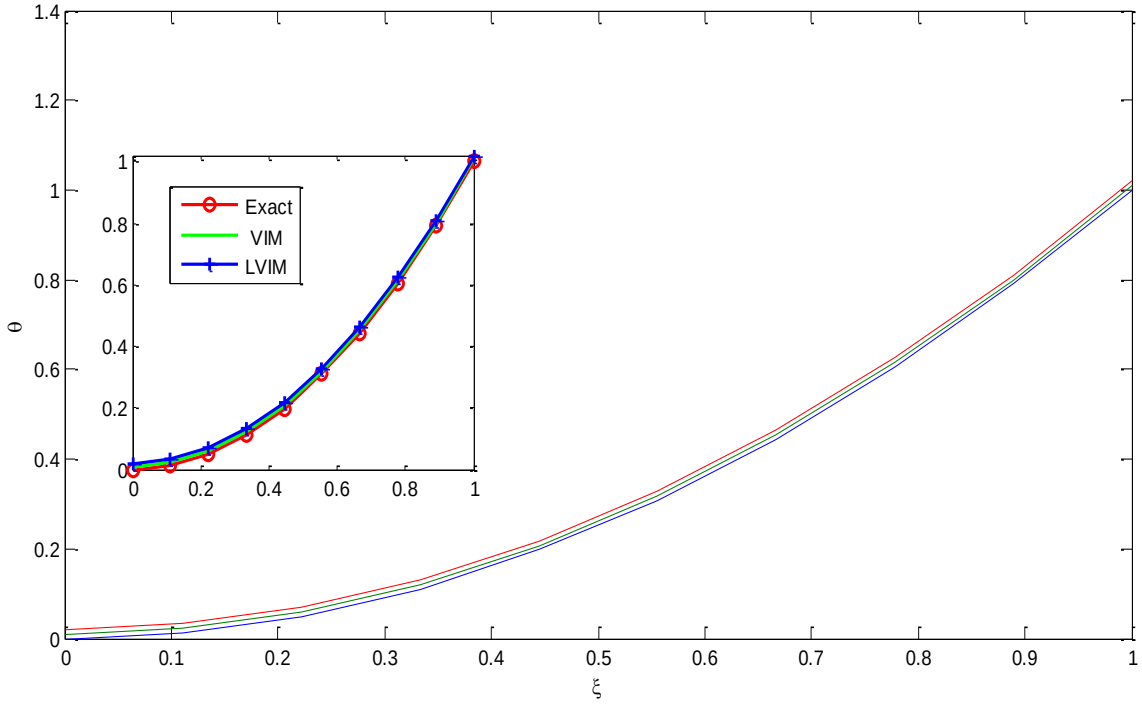

Fig. 2b. Temperature distribution against Non-dimensional length for Exact-, Vim-, and Lvim methods

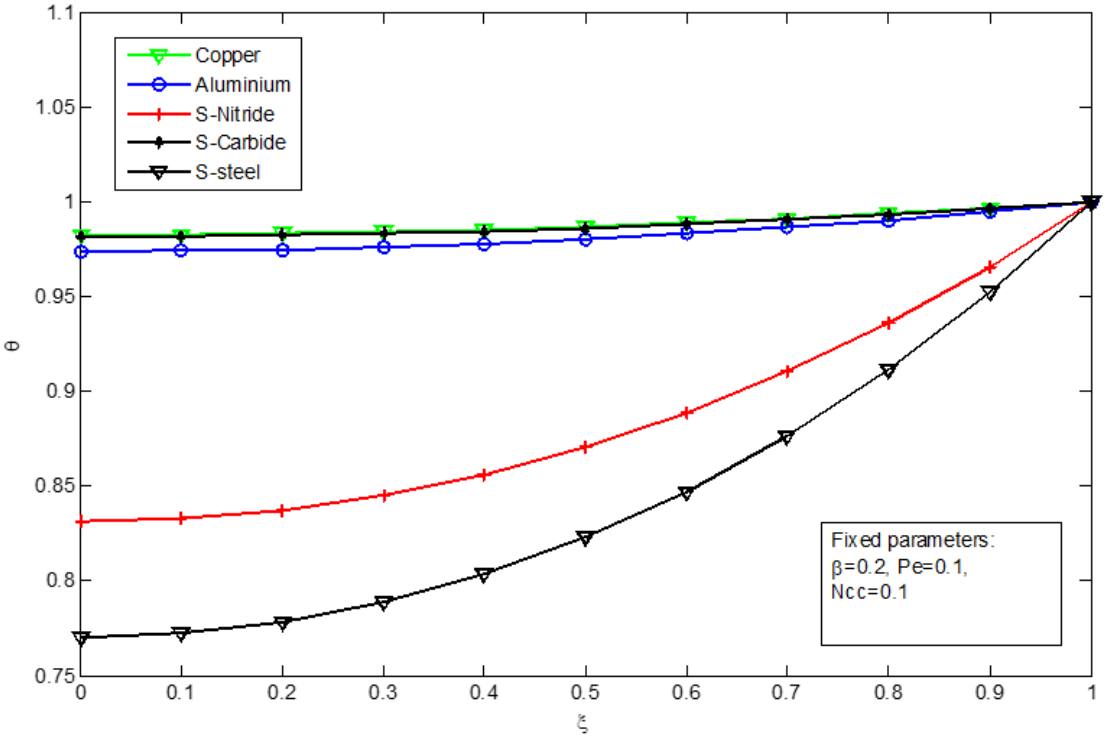

Fig. 3. Effect of Porous materials on Non-dimensional Temperature distribution in a moving fins

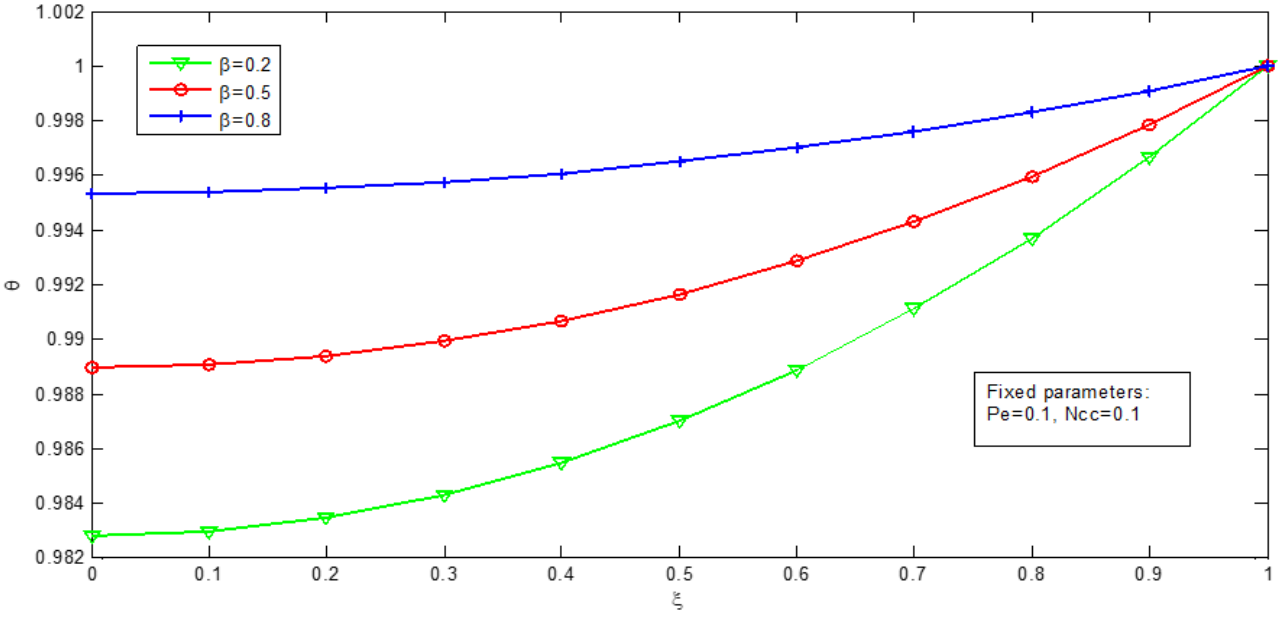

Fig. 4. Effect of varying thermal conductivity parameters (β) on temperature distribution in a copper Porous moving fin.

Accordingly, the curve shows that silicon carbide materials displayed a very close thermal response characteristics with copper material and may be used as a close substitute in areas where copper materials are rarely found. Aluminum material also displayed good thermal response compared to the two materials mentioned above while silicon-nitride materials and stainless- steel materials displayed relatively low thermal response as compared with the three materials earlier mentioned, based on their relative thermal conductive values as displayed in Table 1.

In Fig.4 above, the effect of varying thermal conductivity parameters on non-dimensional temperature distribution in a copper moving Porous fin is demonstrated. The trend shows an expected increasing rise in non-dimensional temperature distribution with increase in thermal conductivity parameter.

The effect of varying Peclet number on non-dimensional temperature distribution in a silicon carbide Porous fins is shown in Fig. 5, below. Since Peclet number is the ratio of Thermal advective transport rate to thermal diffusion transport rate, it is therefore expected that an increase in Peclet number translates to increase in the movement of the fins, thereby reducing the time for heat dissipation, the heat retention in the fin consequently leads to the rise in the non-dimensional temperature distribution.

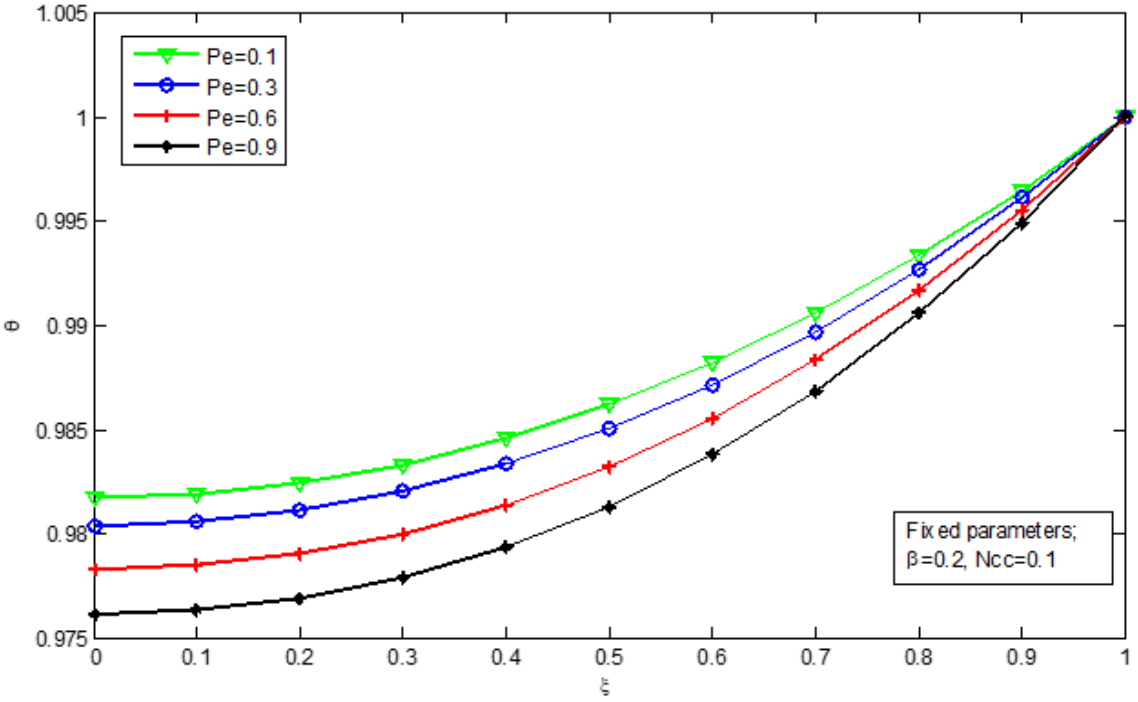

Fig. 5. Effect of varying Peclet number on temperature distribution in a silicon carbide moving Porous fin.

Fig. 6, presents the effect of varying convective-conductive parameter on non-dimensional temperature distribution in a silicon nitride moving porous fin. Since convective-conductive parameter is defined as the ratio of convective heat loss to conductive heat transfer in the porous fin, therefore, as the convective-conductive parameter decreases , the convective

heat dissipation on the surface of the moving porous fin decreases, thereby leading to the rise in non-dimensional temperature distribution.

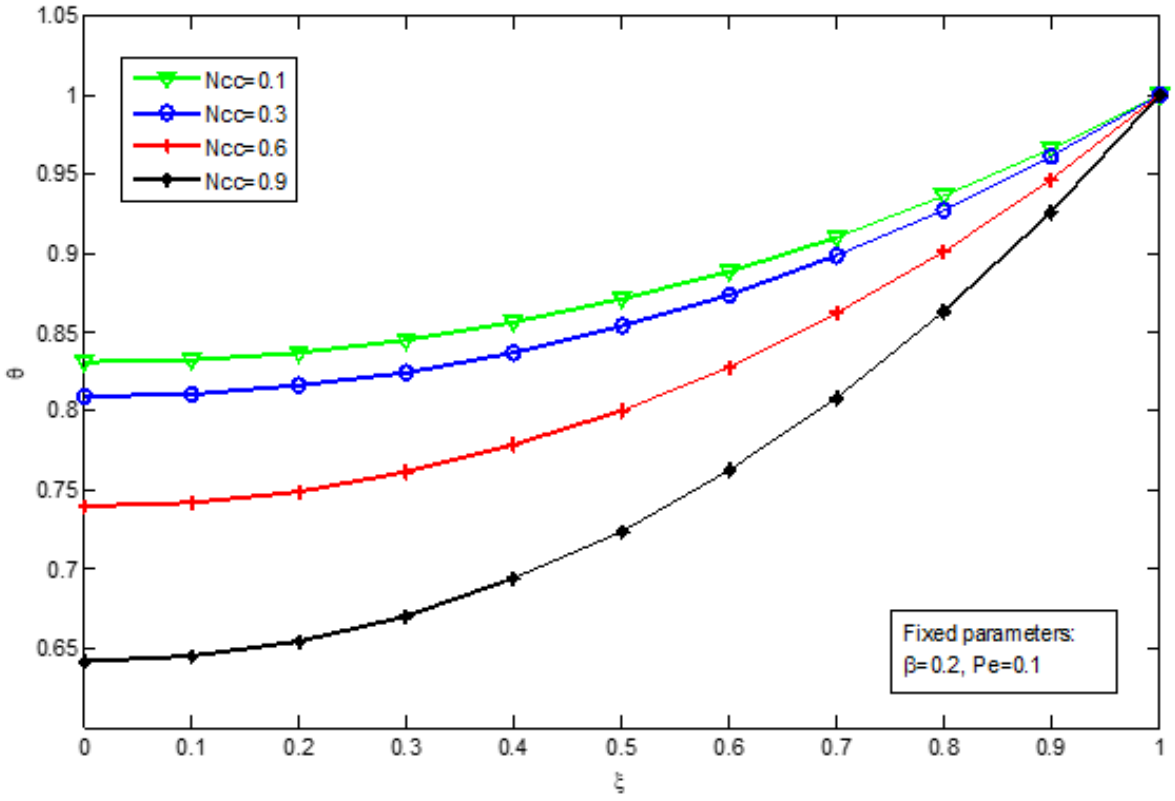

Fig. 6. Effect of varying Convective-conductive term (Ncc) on non-dimensional temperature distribution in a silicon nitride moving porous fin.

In Fig. 7, and Fig. 8, the variation of fin efficiency against Peclet number and convective-conductive parameter are displayed respectively. Fig. 7, shows a decreasing trend in fin efficiency with increase in Peclet number as observed in Fig. 6, that increase in Peclet number leads to rise in non-dimensional temperature distribution due to the reduced time for convective heat dissipation. Hence, the efficiency of the moving porous fin in heat dissipation is reduced. More so, the curve shows copper porous fin as having the least decreasing efficiency with increase in Peclet number, followed closely by silicon carbide- and aluminum- and silicon nitride moving porous fins, while the stainless steel moving porous fin displayed the highest decreasing trend in efficiency with increase in Peclet number. In contrast, the trend in Fig. 8, presents an increase in efficiency of the moving porous fin with respect to increase in the convective-conductive parameter. Since the conductive-convective parameter is directly proportional to convective heat dissipation. Therefore, as the convective-conductive parameter increases, the convective heat dissipation increases, hence an increase in the efficiency of the moving porous fin. Consequently, in respect of thermal conductivity value of each porous fins, copper porous fin shows the highest increase in efficiency with respect to convective-conductive parameter while stainless steel porous fin exhibit the lowest efficiency with respect to increase in convective-conductive parameter.

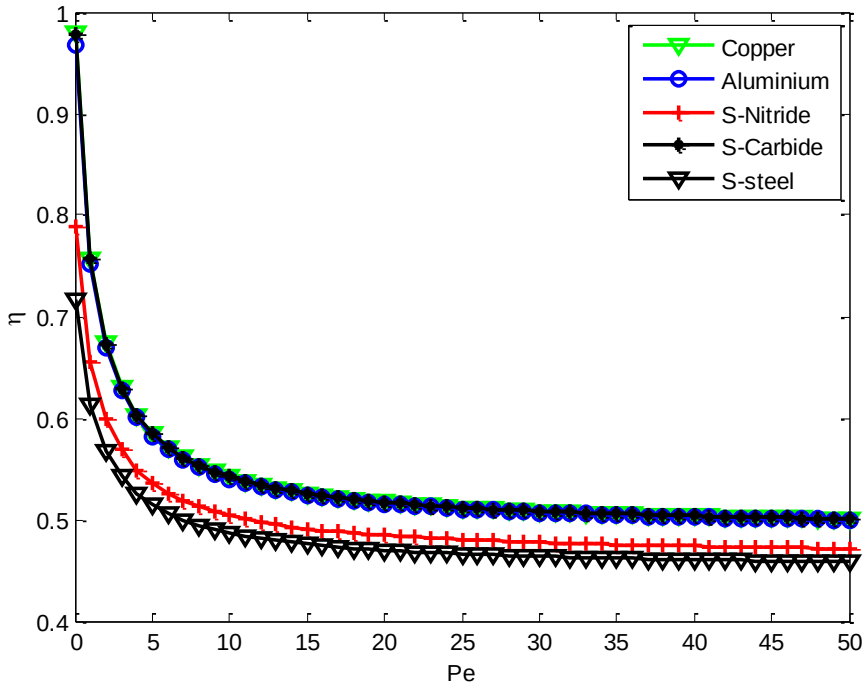

Fig. 7. Material efficiency of porous moving fins with varying Peclect number

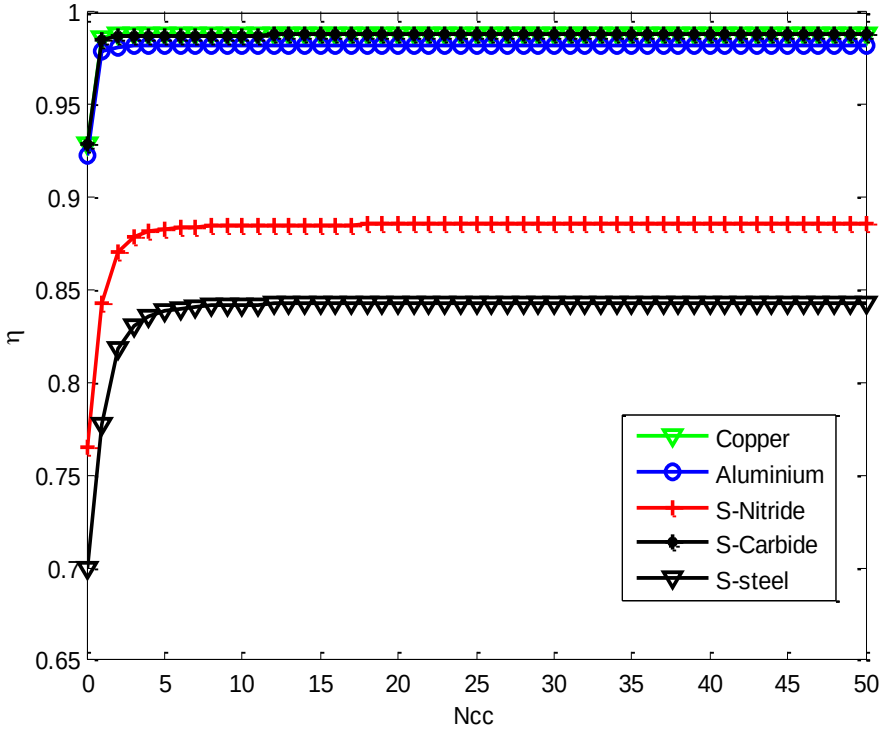

Fig. 8. Material efficiency of porous moving fins with varying convective-conductive term (Ncc)

5. CONCLUSIONS

- Copper-silicon carbide and Aluminum porous fins are most efficient in heat dissipation relative to silicon nitride and stainless steel porous fins.
- The efficiency of moving porous fin shows inverse relationship with Peclet number, but depicted a direct relationship with the convective-conductive parameter.
- The result obtained from Laplace variational iterative method shows high accuracy and agreement with the exact analytical method, which make it an effective tool in analyzing the thermal distribution characteristics of longitudinal fins.

Nomenclature

A unknown constant
A_c cross-sectional Area of the fin (m^2)
h heat transfer coefficient ($W\ m^{-2}\ K^{-1}$)
k thermal conductivity of the materials ($W\ m^{-1}\ K^{-1}$)
k_a thermal conductivity at the ambient fluid temperature ($W\ m^{-1}\ K^{-1}$)
k_b thermal conductivity at the base temperature ($W\ m^{-1}\ K^{-1}$)
L linear differential operator
L Laplace operator
N non-linear differential operator
N_{cc} convective-conductive parameter
P fin perimeter (m)
Pe Peclet number
Q heat transfer rate (W)
S_h Porosity Parameter
T temperature (K)
T_∞ surrounding fluid temperature (K)
T_b base surface temperature (K)
U dimensionless velocity of the moving fin
x distance measured from the fin tip (m)

Greek symbols

β. a constant describing the variation of thermal conductivity
η fin efficiency
ξ dimensionless length of fin
λ Lagrange multiplier
γ the slope of thermal conductivity-temperature curve (K^{-1})
θ dimensionless temperature

Subscript

0 value of x = 0
∞ value at ambient temperature
b value at base temperature
f value of fluid

L value at x = L
s value of solid material

References

[1] D. Q. Kraus and D.A. Kenn. Extended surface heat transfer. In McGraw-Hill, New York, 1972.

[2] P.K. Roy and A. Mallick. Thermal Analysis of straight rectangular fins using Homotopy perturbation Methods. *Alexandrial Engineering Journal,* vol. 55, pp. 2269-2277, 2016.

[3] M. Hatami and D. D. Ganji. Optimazation of the longitudinal fins with different geometries for increasing heat transfer. In ISER 10th International Conference, Kuala Lumpur, Malaysia, 2015.

[4] H. L. Chen and C.C. Wang. Analytical analysis and experimental verification of trapezoidal fin for assessment of heat sink performance and material saving. *Applied Thermal Engineering,* vol. 98, pp. 203-212, 2016.

[5] Purwadi, T. D. Nugroho and P. K. Fin effectiiveness and efficiency with position function of rhombus sectional area in unsteady condition. In *AIP Conference Proceedings*, 1788, 2017.

[6] S. E, Ghasemi, M. Hatami and D. D. Ganji. Thermal analysis of convective fin with temperature dependent thermal conductivity and heat generation. *Case Studies in Thermal Engineering,* vol. 4, pp. 1-8, 2014.

[7] P. Singh, H. Lal and B.S. Ubhi, "Deaign and Analysis of Heat Transfer through fin with Extensions," *International Journal of Innovative Research in Science,* vol. 3, no. 5, 2014.

[8] Y. Reddy, P. Kumar, D. Shrinivasulu and S. Rao. Temperature Distribution Analysis of Pin Fin by Expemental and Finite Element Methods. *Internal Journal of Innovative Research in Science and Engineering and Technology,* vol. 4, no. 10, 2015.

[9] A. S. Joel, U. A. El-Nafaty, Y. I. Makarfi, J. Mohammed and N. M. Musa. Study of Effect of Fin Geometry on Cooling Process of Computer Microchips through Modelling and Simulation. *International Journal of Industrial and Manufacturing Systems Engineerig*, vol. 2, no. 5, pp. 48-56, 2017.

[10] S. Wangikar, N, Sattigeri, P. Mastiholi, M. Ankali and S. Peersade. Enhancement of Heat Transfer Through Different Types of Fins, India, 2003.

[11] M. Jain, M, Sankhala, K. Patidar and L. Aukangabadkar. Heat Transfer Analysis and Optimization of Fins by Variation in Geometry. in Procedings of WRFER-IEEEFORUM , Pune India, 2017.

[12] L.C. Thomas, Transaction of ASME. August 1999. [Online]. Available: http://heattransfer.asmedigitalcollection.asme.org. [Accessed 01 12 2018].

[13] S. Kiwan, Effect of Radiative losses on the Heat Transfer in a Porous Fin. *International Journal of Thermal Science* vol. 46, pp. 1046-1055, 2007.

[14] S. Kiwan and O. Zeitoun. Natural Convection in a Cylindrical Annulus using Porous Fins. *International Journal of Numerical Heat Fluid Flow*, vol. 18 (5), pp. 618-634, 2008.

[15] S. Al-Nimr and M. Kiwan. Using Porous Fins for Heat Transfer Enhancement. *ASME Journal of Heat Transfer*, vol. 4123, pp. 790-795, 2001.

[16] T. Patel and R. Meher, A study on temperature distribution, efficiency and effectiveness of longitudinal porous fins by using Adomian decomposition sumudu transform method. *Procedia Engineering*, vol. 127, pp. 751-758, 2015.

[17] J.Ma, Y. Sun and B. Li, A simulation of a combined conductive, convective and radiative heat transfer in a moving irregular porous fins, using spectral element method. *International Journal of Thermal Science*, vol. 118, pp. 475-487, 2018.

[18] M. Hatami and D. D. Ganji. Thermal behaviour of longitudinal convective radiative porous moving fin with different section shapes and ceramic materials. *Ceramic International*, vol. 40, pp. 6765-6775, 2014.

[19] A. Vahabzadeh, D.D. Ganji and M. Abbasi, Analytical investigation of porous fins with variable section in fully conditions. *Case Studies in Thermal Emgineering*, vol. 5 (2015), pp. 1-12.

[20] D. D. Ganji and M. Hatami, Optimization of the Longitudinal fins with different geometries for increasing the heat transfer, In ISER 10th International Conference, Kuala Lumpur, 2015.

[21] M. G. Sobamowo. Comment on 'Homotopy perturbation sumudu transform method for solving convective radial fins with temperature dependent thermal conductivity of fractional order energy equation'. *International Journal of Heat and Mass Transfer*, vol. 76, pp. 162-170, 2014.

[22] A. Patra and S. Saha Ray, Homotopy perturbation sumudu transform method for solving convective radial fins with temperature dependent thermal conductivity of fractional order energy equation. *International communication in Heat and Mass Transfer*, vol. 76, pp. 162-170, 2014.

[23] Zaidi and Z. Shadad, Application of the Optimal Homotopy Asymptotic Method for Fins with Variable temperature surface heat flux. *World Applied Sciences Journal*, vol. 27, no. 12, 2013.

[24] P. S. Ghoshdastidar and A. Mukhopadhyay, Transient heat transfer in a straight composite fin: A numerical solution by ADI. *International Communication of Heat and Mass Transfer*, vol. 16, pp. 257-265, 1989.

[25] A. Bhowmik, P.K. Roy, D.K. Prasad, R. Das and R. Repaka, Predicting geometry of rectangular and hyperbolic fin profiles with temperature-dependent thermal properties using decomposition and evolutionary methods. *Energy Conversion and Management*, vol. 74, pp. 535-547, 2013.

[26] A.M shafei and S. R. Nimr, Heat conduction of a Hollow Cylinder via generalized Hankel Transform, *International Research Journal of Applied and Basic Sciences*, vol. 3(4), pp. 758-769, 2012.

[27] V. Daftardar-Gejji et al., New iterative method: Application to partial differential equations. *Journal of Applied Mathematics and Computation*, vol. 203, pp. 778-783, 2008.

[28] A. Yildirim et al, An efficient new iterative method for finding exact solutions of nonlinear time-fractional partial differential equations. *Nonlinear Analysis Modelling and Control* , vol. 16(4), pp. 403-414, 2011.

[29] S. Xu and X. Su, Steady State Thermal Analysis of a Plate Fin Heat Sink Using Green's Function. *Modern Physics Letter B*, vol. 24(13), 2010, pp. 1495-1498.

[30] U. K. N. A. a. T. M.-D. I. Khan. Thermal radiation effect on squeezing flow casson fluid between parallel disks. *Communication in Numerical Analysis*, vol. 2, pp. 92-107, 2016.